Variation in visual sensitivity predicts motion sickness in virtual reality

Jacqueline M. Fulvio and Bas Rokers

University of Wisconsin–Madison

Author Note

Jacqueline M. Fulvio, Department of Psychology, University of Wisconsin-Madison.

Bas Rokers, Department of Psychology, University of Wisconsin-Madison.

This research was supported in part by funding provided by Facebook Reality and Google Daydream.

Correspondence concerning this article should be addressed to Jacqueline M. Fulvio, Department of Psychology, University of Wisconsin–Madison, WI 53706.

Contact: jacqueline.fulvio@wisc.edu

Abstract

Motion sickness varies across observers. While some experience immediate and severe symptoms, others seem relatively immune. Multiple explanations have been advanced. Some argue that conflicting cues provided by the visual and vestibular systems are the underlying cause. Others claim postural sway, which differs between the sexes, can explain previously-reported motion sickness susceptibility differences. We used virtual reality to test these accounts. We found that an observer's visual sensitivity to motion parallax predicted susceptibility, but found little evidence for differences based on sex (N = 95; 59 females, 36 males). Furthermore, our results suggest that sex differences are likely due to poor personalization of VR displays, which default to male settings and introduce cue conflicts for the majority of females. These results suggest that the probability of detecting cue conflicts is limited by an observer's sensitivity to specific sensory cues and thus identify a cause for differences in motion sickness severity.

Keywords: Motion sickness, Visual sensitivity, 3D Motion perception, Motion parallax, Virtual reality

Variation in visual sensitivity predicts motion sickness in virtual reality

Although the visual system is often studied in relative isolation, it has clear connections to other components of the nervous system, for example in the regulation of diurnal rhythm, arousal and balance. One area where this connection becomes apparent is in the domain of motion sickness. Conflicting sensory input from the visual and vestibular systems can lead to sometimes severe discomfort. While the connection between sensory conflict and motion sickness has been clearly established, and is painfully apparent to anyone who has experienced car or sea sickness, an account for the considerable individual variation in susceptibility to motion sickness has been more elusive.

Several theories have been advanced to explain motion sickness specific to virtual environments (see LaViola (2000) for a review). Cue conflict theory posits that motion sickness is the result of conflict between sources of spatial information that are typically in concert (Reason, 1978). Although these conflicting sources may arise within a modality, such as visual input (Keshavarz et al., 2011), the conflicting sources have largely been attributed to cross-modal inputs to the visual and vestibular systems (e.g., Reason & Brand, 1975; Reason, 1978; Oman, 1990; Howarth & Costello, 1997; Akiduki et al., 2003; Nishiike et al., 2013). From an evolutionary perspective, such conflicts were likely to occur following the ingestion of neurotoxins. Thus, the body's nausea and vomiting responses, which cause the toxin to be expelled, may have developed as the result of an evolutionary adaptation (Money, 1990; Treisman, 1977; Bronstein et al., 2013; Lackner, 2014).

Two observations provide additional support for the sensory cue conflict theory. First, motion sickness does not occur in individuals who lack a vestibular system. Second, those with a dysfunctional vestibular system are particularly susceptible (Paillard et al. 2013). In individuals

with a functioning vestibular system, a relationship between vestibular sensitivity to self-motion and symptoms of motion sickness has been established, although it is often small and context-specific (Kennedy and Graybiel 1965). Furthermore, to our knowledge, a relationship between *visual* sensitivity and motion sickness has not been established.

An alternative explanation is offered by postural instability theory. It posits that motion sickness is not due to an evolutionary adaptation, but is instead due to an inability to regulate postural sway (Riccio and Stoffregen 1991). A number of studies report that greater postural sway precedes the onset of motion sickness symptoms in both physical environments (Smart et al. 2002), video games (Stoffregen et al. 2008), and virtual reality headsets (Munafo et al. 2017).

A second claim made by advocates of the postural instability theory is that postural sway is inherently larger in females than males. Consequently, the theory predicts that females should exhibit a greater propensity for motion sickness. Indeed, some prior work has found evidence for such sex differences in motion sickness susceptibility (Munafo et al., 2017; Allen, Hanley, Rokers, & Green, 2016)

However, the relationship between postural sway and motion sickness is not consistent, occurring in some but not all of the reported experiments. Moreover, some studies have called the role of postural sway as a direct cause of motion sickness into question, instead suggesting that changes in sway occur at the same time as motion sickness onset (Nachum et al., 2004; Akizuki et al., 2005; Nishiike et al., 2013).

To adjudicate between these two alternative theories, we designed a series of experiments. In our experiments, we tested individual observers' sensitivity (both males and females) to various cues that signal object motion. We chose to manipulate sensory cues pertaining to object motion in depth based on the general equivalence between an observer

moving through an environment and objects moving around an observer. Prior work has identified considerable variability in the sensitivity to visual cues that specify object motion. For example, observers exhibit independent sensitivity to interocular velocity differences (IOVD) and changing disparities (CD) (Allen et al., 2015). To measure susceptibility to motion sickness, the same observers watched video footage containing cue conflicts in a virtual reality headset while we measured body sway. We then determined the relationship between sensitivity to various sensory cues and motion sickness due to video viewing.

To summarize our logic, we examined inter-individual differences in sensitivity to specific motion in depth cues as predictors of motion sickness. We reasoned that both the vestibular and visual systems provide estimates of the degree of self-motion. If these estimates tend to be highly accurate, then the system should be more likely to detect mismatches between the estimates. Therefore, observers who are highly sensitive to these cues should be more susceptible to motion sickness, while observers with poor sensitivity should be less susceptible. On the other hand, if motion sickness has little to do with cue conflict, and postural instability theory holds, we should instead see a clear relationship between sex and severity of motion sickness symptoms.

We found that the sensitivity to, and reliance on, specific sensory cues to 3D motion is related to individual susceptibility to motion sickness. In particular, individual sensitivity to motion parallax cues produced by small head movements predicts the severity of motion sickness symptoms. At the same time, we found little evidence for a relationship between sex and motion sickness symptoms, although we did find evidence that observers self-regulate discomfort by modulating their head movement over time.

We subsequently explored a potential cause for previously reported sex differences. Default VR settings tend to be geared toward the average male. Deviations from the default will introduce cue conflicts into the visual display, and such deviations are of course much more likely for females. Having tailored the display to the interpupillary distance (IPD) of each individual observer, we did not find differences in motion sickness susceptibility based on sex in our sample of observers.

We conclude that motion sickness may be reduced in VR by providing settings personalized to the individual observer, minimizing specific sensory cues, or reducing an observer's sensitivity to that cue, by perhaps counter-intuitively degrading visual fidelity.

Methods

Observers

108 observers gave informed written consent to complete the study. A total of 103 successfully completed all parts of the study. Five observers did not complete the experiment due to technical issues (n = 3), experimenter error (n = 1), or difficulty seeing the stimuli (n = 1). Data from 8 out of the remaining 103 observers who successfully completed all parts of the study were excluded because they did not achieve performance above chance level in any condition on the psychophysical task - see "3D motion discrimination task" section below. Therefore, data from a total of n = 95 observers were included in the main analyses. The sample size was based on that used in a previous study that investigated motion sickness propensity in virtual reality (Allen et al., 2016). The experiments were approved by the IRB at the University of Wisconsin-Madison. Observers received course credit in exchange for their participation.

Display Apparatus

Observers viewed visual stimuli in the Oculus Rift Development Kit 2 (DK2; www.oculusvr.com), a stereoscopic head-mounted virtual reality system (see **Fig**. **1**, “Virtual reality headset” panel) with a 14.5 cm low-persistence AMOLED screen (Samsung) - embedded in the headset providing a resolution of 1920x1080 pixels (960x1080 pixels per eye) with a refresh rate of 75 Hz. The horizontal field of view of the device is about 85 deg (100 deg diagonal). The device utilizes six degrees of freedom (6 DoF) head-tracking for head-motion contingent updating of the display. Positional tracking was achieved at 60 Hz with .05 mm precision via an external camera with a near-infrared CMOS sensor. Tracking of head rotation was achieved at 1000 Hz with .05 deg precision via an accelerometer, gyroscope, and magnetometer embedded in the headset. The effective tracking latency after sensor fusion was about 2 ms and head-movement-to-photon latency was about 14 ms.

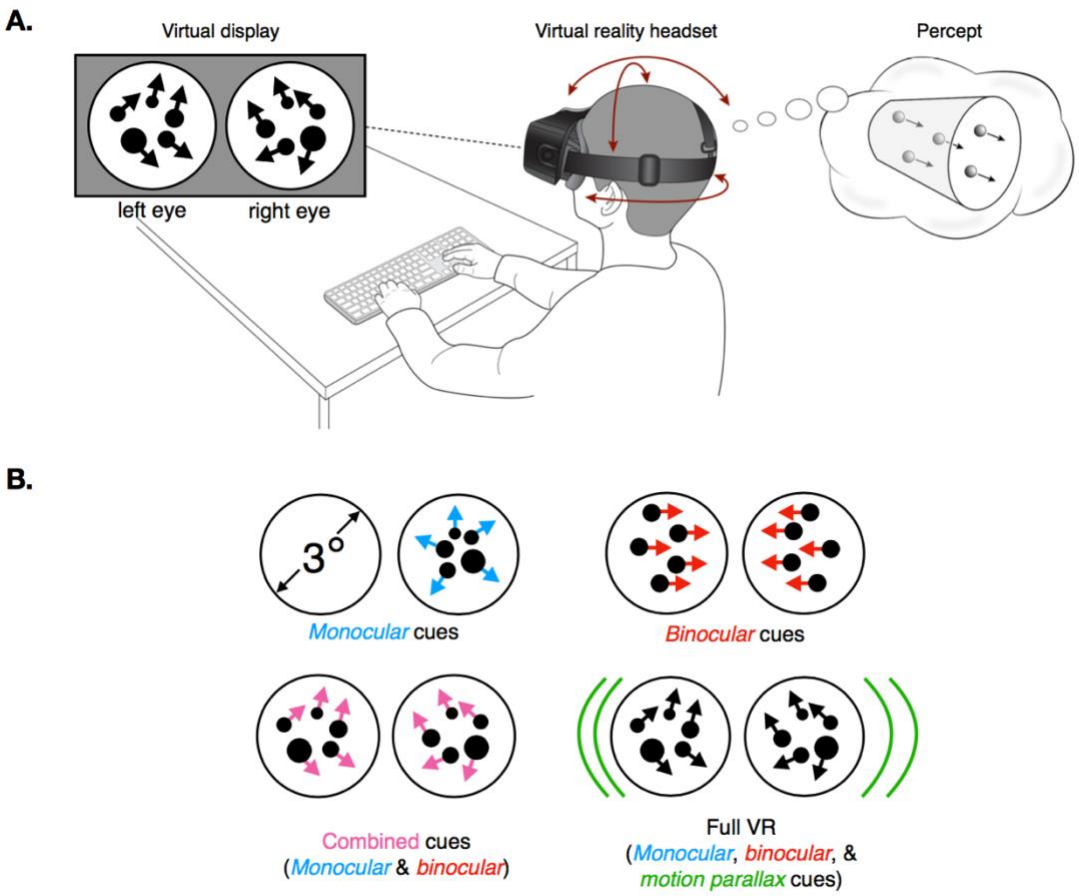

Figure. 1. Experimental details. A. "Visual display": Illustration of left- and right-eye stimulus elements as presented in the motion task. The illustration depicts the random dot stimulus. In the actual experiment, the dot stimulus was comprised of 12 dots whose properties varied according to the sensory cue condition (see B. for more details). The dots were visible within a circular aperture in a flat surface positioned at the fixation distance of the display. "Virtual reality headset": Seated observers viewed the stimuli in an Oculus DK2 head-mounted display. Their head movements were tracked (6 degrees of freedom) and recorded in all conditions. Depending on the experimental condition, the virtual scene updated according to the head movements. "Percept": Illustration of the experimental response paradigm. Observers fixated the center of the circular aperture. The random dot stimulus would appear at fixation and randomly move towards or away with a random coherence for 250 ms before disappearing. Observers indicated the

perceived direction of motion by button press. Observers were given unlimited time to respond. Subsequently, both visual and auditory feedback were provided: the percent correct up to and including the current trial was displayed at fixation and an appropriate sound was played. **B.** Illustration of the four sensory cue conditions tested in the motion task. In the Monocular cues condition, the dot stimulus was randomly presented to one eye on each trial. The dots changed in size and density according to their motion direction. In the Binocular cues condition, binocular disparity and interocular velocity change cues were present, and size and density cues were removed. In the Combined cues condition, binocular disparity and interocular velocity change cues as well as dot size and density cues were present in the stimulus. In the Full VR condition, all of the cues in the Combined condition were also present, as well as motion parallax cues due to head-motion contingent updating of the display.

The display was calibrated using standard gamma calibration procedures. Minimum and maximum display luminances were <0.01 cd/m2 and 64.96 cd/m2, respectively. The experiment was controlled by MATLAB and the Psychophysics Toolbox (Brainard 1997; Kleiner et al. 2007; Pelli 1997) on a Macintosh computer and projected on the display of the DK2 headset. During the psychophysical task portion of the study (see next section, “3D motion direction discrimination task”), observers used a keyboard to initiate trials and make responses.

Experimental Procedure

Each observer completed a single 1-hour experimental session. After observers gave informed consent, their static stereoacuity was measured using the Randot Stereotest (Manufacturer, Location). All but two observers met the criterion of reaching level 5 (70 arc sec) on its graded circles test. The remaining two observers achieved a level of 4 (100 arc sec), but

were included in subsequent data analyses after statistical tests demonstrated that their performance did not differ from the remaining sample. The inter-pupillary distance (IPD) was then measured for each observer using a pupillometer (Essilor Instruments, USA), providing measures in half-millimeter increments. Observers next completed the Simulator Sickness Questionnaire ("baseline SSQ"; (Kennedy et al. 1993)). Upon completion of the questionnaire, observers underwent a brief calibration procedure in which the DK2 HMD was calibrated for their IPD and height. They were then introduced to the experimental task and completed 50 practice trials (see "Motion task" section below for more details) in the presence of the experimenter.

The experiment then began with the sensitivity assessment, which we describe in more detail below. Observers completed four 2.5-minute blocks of the motion task in a random, counterbalanced order across observers. Observers took brief breaks between these blocks, during which they completed the SSQ ("post task"). After the final block and SSQ, observers entered the motion sickness phase of the experiment. They watched up to 22.5 min of stereoscopic video content with the option to quit if the experience became intolerable. Upon completion of the video content (or quitting the viewing), observers completed another SSQ ("post video"). In the final five minutes, observers were asked to completed a brief questionnaire reporting on their experience with motion sickness and virtual reality prior to our experiment, and they were debriefed about the study. Prior to leaving, they completed a final SSQ ("end of session").

Motion Task

The sensitivity assessment was based on observers' performance on a 3D motion direction discrimination task. Observers judged the motion direction of a set of 12 white dots

0.02 cm in diameter at a 1.2 m fixation distance (**Fig. 1A**, “Virtual display” panel). The dots appeared at the center of a visual scene and moved toward or away from the observers with a variable level of motion coherence, pseudo-randomly sampled in equal proportion from [0% 16.67% 50% 100%] coherence for 13 of the observers, and from [16.67% 50% 100%] for the remaining 82 observers. Dots were presented for 250 ms and subsequently disappeared.

We manipulated motion coherence by varying the proportion of signal to noise dots. On each stimulus frame, we randomly selected a subset of dots as signal dots, which moved coherently, either toward or away from the observer (perpendicular to the screen). The remaining dots (noise dots) were given random *x*, *y*, and *z* coordinates. Signal and noise dots were selected on a frame-by-frame basis to help prevent observers from tracking the direction of motion of individual dots. Direction of motion (i.e., “toward” or “away”; see **Fig. 1A**, “Percept” panel) was chosen pseudo-randomly on each trial.

Multiple visual cues signal motion in depth (Beverley & Regan, 1973; Brenner et al. 1996; Nefs et al., 2010). We aimed to quantify observer sensitivity to each cue by manipulating the available cues in the dot motion stimulus. We tested sensitivity in four conditions: *Monocular cues* (dot size and density changes presented to one eye only), *Binocular cues* (containing binocular disparity and inter-ocular velocity differences, but lacking the monocular cues of dot size and density changes), *Combined cues* (containing both the monocular and binocular cues), and *Full VR* (containing the combined cues as well as motion parallax cues due to head movement) (see **Fig. 1B** and see **Supplemental Material** for videos illustrating the four cue conditions). It is important to note that in the Monocular condition, the dots were presented to one, pseudo-randomly chosen, eye on each trial.

The motion stimuli were presented in the center of a virtual room (3 m in height, 3.52 m in width, and 3.6 m in depth). While this room served no function during the actual experiment, it helped observer immersion during initial instruction. The virtual wall, ceiling, and floor were all mapped with different tiled textures to facilitate better judgment of distances throughout the virtual space, and judgment of the stimulus motion trajectories. The room contained a surface that was positioned at the display's focal distance (1.2m from the observer). The plane was textured with a 1/f noise pattern that aided accommodation and vergence. Stimuli were presented in a 3 deg radius circular aperture located in the center of the surface with the dots confined to the central 2.4 deg to prevent occlusion by aperture's edge. A small (0.04 deg) white fixation dot was visible in the center of the aperture at all times except when a dot motion stimulus was presented. All stimulus elements were anti-aliased to achieve subpixel resolution.

Observers were instructed to report the dot motion direction. Observers indicated the direction of dot motion by pressing the up arrow key on the keyboard for receding motion and the down arrow key for approaching motion. In recent work, feedback was shown to be critical for the recruitment of sensory cues in VR displays, especially binocular and motion parallax cues to motion-in-depth (Fulvio and Rokers 2017). Likewise, to encourage recruitment of the sensory cues in the different conditions in the current study, observers received auditory feedback (a "cowbell" sound on correct trials and a "swish" sound on incorrect trials) as well as visual feedback (behavioral performance up to and including the current trial in terms of percent correct was displayed at the fixation point). If the most recent response was correct, the performance was displayed in green; if incorrect, in red.

During stimulus presentation, observers were asked to keep their heads still and maintain fixation. In all but the Full VR condition, head movement had no effect on the display, so that it

appeared to the observer that the virtual environment was “glued” to the head. In the Full VR condition the visual display updated according to head movement, so that it appeared that the observer was present in a stationary immersive virtual environment.

Observers completed the task in four 2.5-minute blocks after completing 50 practice trials with feedback in the Full VR cue condition. Observers that were presented with 4 coherence levels completed 84 trials, and observers that were presented with 3 coherence levels completed 90 trials with each of the blocks. All observers completed four blocks in a randomized, counterbalanced order. Each block contained stimuli from one of the four cue conditions (Monocular, Binocular, Combined, or Full VR). Between blocks, observers took short breaks during which they removed the VR headset and completed the Simulator Sickness Questionnaire (see “Quantifying motion sickness” section below).

Video Content

Observers viewed up to four stereoscopic videos (Allen et al., 2016), totaling ~22.5 min in the VR headset, played in Windows Media Player. The four videos increased in level of intensity: (1) a 5:34 min, first-person video of a car driving through mild traffic, (2) a 3 min first-person computer-generated (CG) video of a fighter jet flying through a canyon, (3) a 6:26 min first-person video of a drone flying through a parking lot, and (4) a 7:19 min first-person video of a drone flying around a bridge (see **Fig. 2** for stills from the four videos). All observers watched the videos in the same order. Observers were told they could stop viewing the videos if and when the experience became intolerable. The total viewing time was recorded for each observer.

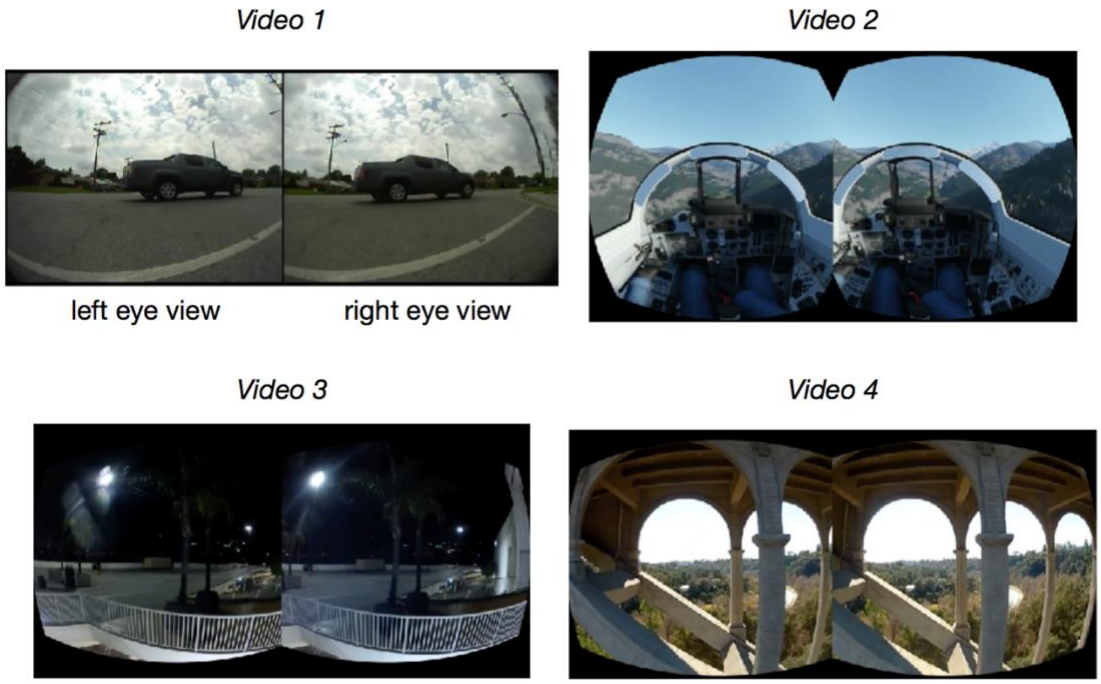

Figure. 2. Stills from motion sickness inducing videos. After completing the four blocks of the motion task, all observers viewed up to four videos while wearing the Oculus DK2 head-mounted display in the same order (up to 22.5 minutes). The videos increased in intensity, and observers were given the option to quit if viewing became intolerable. All observers, whether they stopped the video viewing early or not, completed the Simulator Sickness Questionnaire (SSQ) to indicate the severity of motion sickness symptoms.

Data Analysis

Quantifying Sensitivity

For each cue condition, we calculated the percentage of ‘toward’ responses as a function of direction and motion coherence. Standard error of the mean (SEM) was calculated based on the binomial distribution of the (toward/away) responses. We fit the percentage of toward

responses *g(x)* as a function of direction and motion coherence (*x*) with a cumulative Gaussian using nonlinear least squares regression using the lsqcurvefit function in MATLAB:

$$g(x) = \frac{1}{2}\left[1 + \mathrm{erf}\left(\frac{x-\mu}{\sigma-\sqrt{2}}\right)\right] \quad (1)$$

where μ is the estimate of observer bias, and σ reflects the precision of the responses for the respective sensory cue condition. To stabilize fits when precision was low, we enforced a bound of ±33% on μ and bounds of [0.01 100] on σ. Sensitivity was computed as 1/σ.

To determine if performance for each cue condition was different from chance, we simulated performance of an observer who responded randomly on each trial for 90 total trials for 3 coherence levels and 84 trials for 4 coherence levels. We then bootstrapped the sensitivity confidence interval. At the 95% confidence level, the upper sensitivity bound was .49/.43 for the conditions with 4 and 3 coherence levels, respectively. If an observer's performance did not exceed these bounds, (i.e., perform above chance level) in any of the four conditions, the observer was excluded from further analyses (n = 8).

Quantifying Motion Sickness

To quantify motion sickness, observers completed the SSQ at six separate time points during the experimental session (see "Experimental Procedure" above). Observers rated the severity of 16 symptoms as "none", "slight", "moderate", or "severe", which were then numerically scored as 0, 1, 2, and 3, respectively. The symptoms form three subscales: (1) nausea (N) ranging from 0 - 200.34, (2) oculomotor disturbances (OD) ranging from 0 - 159.18, and (3) disorientation (D) ranging from 0 - 292.32. The severity of symptoms on each of the three scales was computed via standardized formulas (see Kennedy et al., 1993), which were then combined using a final formula to produce an overall ("Total") sickness score ranging from

0 - 235.62. Larger scores correspond to more severe symptoms on all scales. Although the sickness scores were computed for each of the six questionnaires completed by each observer during the experimental session, we were primarily interested in the effects of the video viewing. To quantify the impact of video viewing on sickness levels, we computed the change in motion sickness from before the video viewing (based on the "post task" SSQ) to after the video viewing ("post video" SSQ).

Quantifying Head Jitter

Head movements during the task were very small due to the presentation of the stimulus at fixation for a brief time - we therefore refer to these small head movements as "head jitter" (Fulvio and Rokers 2017). We analyzed translational head jitter and rotational head jitter based on the 6 DoF head tracking built into the DK2 headset. For each block of the motion task, a single continuous head trace was saved, containing the 4x4 model view matrix for each eye at every screen refresh (75 Hz or ~13.33 ms). We inverted the model view matrix and determined the "cyclopean" view matrix at each time point based on the midpoint between the two eyes' views. From these traces, we extracted the time points that corresponded to each individual trial in order to analyze the head movement on a trial-by-trial basis. No additional transformations were applied.

To quantify translation, we computed the head's path length through 3D space ('translational jitter') for each trial. We path-integrated the translation of the head by summing the Euclidean distance between each consecutive head position obtained from the X, Y, and Z components of the "cyclopean" view matrix. Point-to-point estimates ≥ 0.002 m (which corresponded to a velocity ≥ 0.15 m/s) were excluded because they were unrealistically large and likely reflected tracking errors (~9.5% of all time points across all observers, conditions, and

trials). Thus, when an erroneous tracking time point was identified, the path integration ignored that point. Because the distributions of translational jitter were typically positively skewed, we computed the median translation for each observer. Average translational jitter was then computed across observers.

Similar methods were used to quantify rotation. We first computed the total angular distance that the head rotated in 3D space on each trial ('rotational jitter'). To do so, we extracted the rotation components (i.e., the first 3 rows and columns) from the 4x4 "cyclopean" view matrix *M*. *M* was then decomposed to determine the amount of rotation about each axis in the following order: y (yaw), z (roll), and x (pitch). To calculate the total rotation, the observers' orientation at the start of the trial was represented by the vector (0, 0, 1), which corresponded to the observer looking straight ahead. Following time point 1, the direction vector at each time point was calculated by computing the dot product of *M* and the starting vector (0, 0, 1). Total rotational jitter was computed by summing the total head rotation between every two adjacent time points (i.e., the absolute angle between two successive vectors). Point-to-point estimates of rotation that were ≥ ~28.5 arcmin (which corresponded to an angular velocity of ~36 deg/s) were excluded (<1% of all time points across all observers, conditions, and trials). As with the computation of translational jitter, when an erroneous tracking time point was identified, the path integration ignored that point. Rotational jitter distributions were typically positively skewed, so we computed the median rotation for each observer. Average rotational jitter was then computed across observers.

Statistical Analysis

The relationship between sensitivity in each stimulus condition and motion sickness due to video viewing were quantified through an analysis of variance (ANOVA) evaluated on

general linear model fits to the individual subject data for each of the sensory cue conditions with sensitivities (1/cue) included as a fixed effect and subject included as a random effect. Individual sensitivity values that were 3 standard deviations beyond the mean in each of the cue conditions were excluded from the analysis, yielding: n = 95, 93, 94, 94 data points included in the model for the Full VR, Combined, Monocular, and Binocular, respectively. A Bonferroni-corrected alpha level of .0125 was used to test for significance of the four relationships.

To assess the relationship between sensitivity to motion parallax and motion sickness, we computed an index that quantified an observer's sensitivity to motion parallax separate from sensitivity to the other cues that specified 3D motion. Specifically, we computed the difference between sensitivity in the Full VR condition and the average of the sensitivity in the other three conditions (Monocular, Binocular, and Combined). We then quantified the relationship between this difference and motion sickness due to video viewing by an ANOVA evaluated on the general linear model fit to the individual subject data with difference in sensitivity included as a fixed effect and subject included as a random effect. Significance was evaluated at the alpha = .05 level.

The role of sex in the relationship between sensitivity to the cues in the Full VR condition and motion sickness due to video viewing was evaluated through an ANOVA evaluated on general linear model fits to the individual subject data with sensitivity to the Full VR condition (1/Full VR) and sex included as fixed effects along with their interaction and subject included as a random effect. Significance of the main effects and the interaction was evaluated at the alpha = .05 level.

Patterns of head jitter were analyzed over time. For each observer, head jitter was averaged for each trial over the four blocks of the motion task (i.e., the sensitivity assessment

portion of the experiment), giving a within-subject mean head translation (in mm) and within-subject mean head rotation (in arcmin) for each trial. We fitted linear, quadratic, and power models to the between-subject mean head translation and between-subject mean head rotation across trials, with the first 5 trials omitted to ensure stable behavior at the start of the trial. An AIC model comparison indicated that the quadratic model best-characterized the pattern of head translation and rotation across trials and subjects. We then carried out two multiple quadratic regressions, one for translational head jitter and one for rotational head jitter. These models tested for an effect of average observer sensitivity to the sensory cue conditions on head jitter, controlling for trial (i.e., time spent in the device) with subject included as a random effect. N = 8075 total data points per head jitter type were supplied to the model, however, outliers that were 3 standard deviations beyond the mean at each time point (i.e., trial) were excluded for consistency with other analyses (~1% & ~2% of all data points for translational and rotational head jitter, respectively). This exclusion did not change the overall results or their interpretation. Significance of the effect of sensitivity was evaluated at the alpha = .05 level.

Results

Variability in Sensitivity to 3D Motion Cues in VR

We first assessed sensitivity to 3D motion cues in virtual reality. Each observer judged the direction (toward/away) of a cloud of dots moving with variable coherence levels. We fit a cumulative Gaussian to the observer's performance and used the inverse of the standard deviation ($1/\sigma$) as an estimate of the observer's sensitivity. Each observer's motion sensitivity was tested in four cue conditions (Monocular, Binocular, Combined, and Full VR). Combined stimuli contained both Monocular and Binocular cues, and Full VR stimuli contained the Combined cues as well as motion parallax cues.

We found considerable variability in sensitivity to the different sensory cues (**Fig. 3**). Cue sensitivity varied both within and across observers. On average sensitivity was greatest when more cues were available (Full VR and Conditions), and smallest when fewer cues were available (Monocular and Binocular Conditions), and binocular cue sensitivity was generally weakest. However, observers with lower sensitivity in one sensory cue condition were not necessarily those with lower sensitivity in the other conditions. Importantly, variability among observers *within* each sensory cue condition was larger than the variability in sensitivity *between* the four cue conditions. These effects do not appear to be related to stereoacuity as RANDOT performance did not predict sensitivity in any of the cue conditions ($p > .05$ for all conditions).

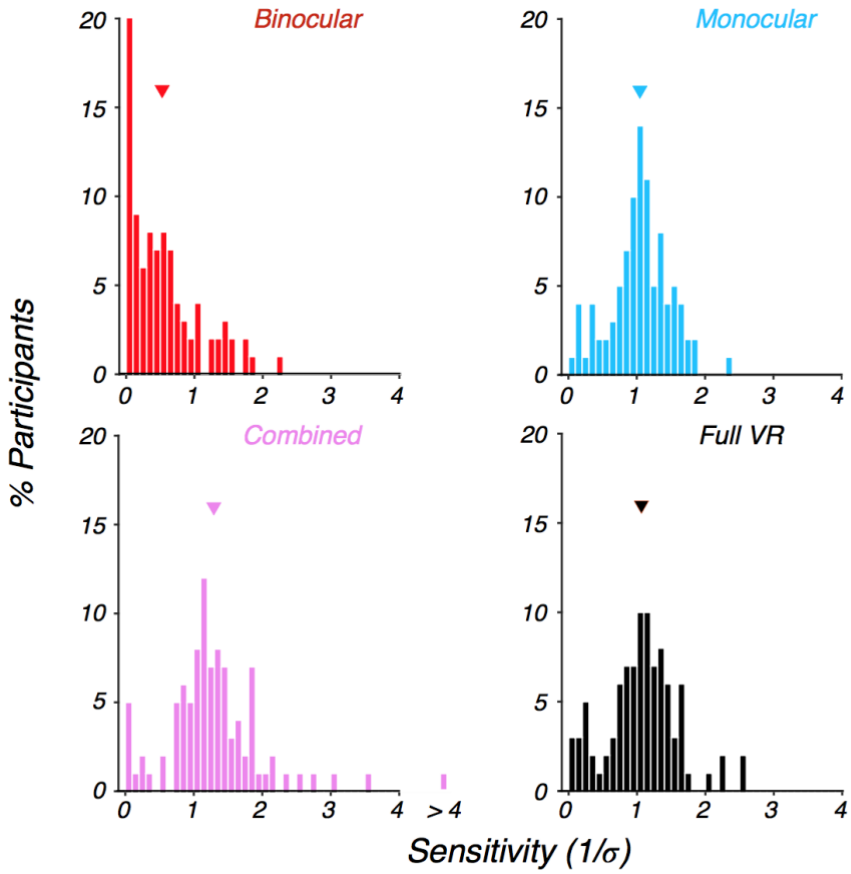

Figure. 3. Sensitivity to 3D motion cues varies across observers. On average sensitivity is greatest when more cues are available (Full VR and Conditions), and smallest when fewer cues are available (Monocular and Binocular Conditions), with binocular cue sensitivity being particularly poor. However, variability among observers within each sensory cue condition was considerably greater than the variability in sensitivity between the four cue conditions, indicating considerable inter-observer sensitivity differences to each cue. Each panel reflects the distribution of sensitivity to the particular cue condition across n = 95 observers. Bars in the histograms correspond to the % of participants falling in each sensitivity bin, and the triangles correspond to the between-subject mean sensitivity for the condition.

VR Video Content Induces Motion Sickness

We next assessed the propensity for motion sickness in the same observers using the Simulator Sickness Questionnaire (SSQ; (Kennedy et al. 1993)). This questionnaire was developed to quantify the symptoms most commonly experienced by users of virtual reality systems and has been normed to provide scores on three categorical scales. Larger scores indicate more intense motion sickness symptoms. Observers completed the SSQ at several points in time throughout the study (see Methods for more details): 1. after consenting to participate in the study, prior to any VR exposure ("baseline"); 2. immediately after the motion task, prior to viewing the video content ("post task"); 3. immediately after viewing the video content ("post video").

Observers generally reported little sickness at the beginning of the study (**Fig. 4,** blue bars). Slight increases in motion sickness symptoms were reported after completion of the motion task (red bars). We saw a considerable increase in motion sickness post video viewing, producing moderate levels of motion sickness on average, confirming that our manipulation of motion sickness had its intended effect (yellow bars). Of note, as with the results of the sensitivity assessment (i.e., performance in the motion task), there was considerable variability across observers in the intensity of motion sickness symptoms throughout the study, with some individuals appearing highly-sensitive to the manipulation and others apparently insensitive to it.

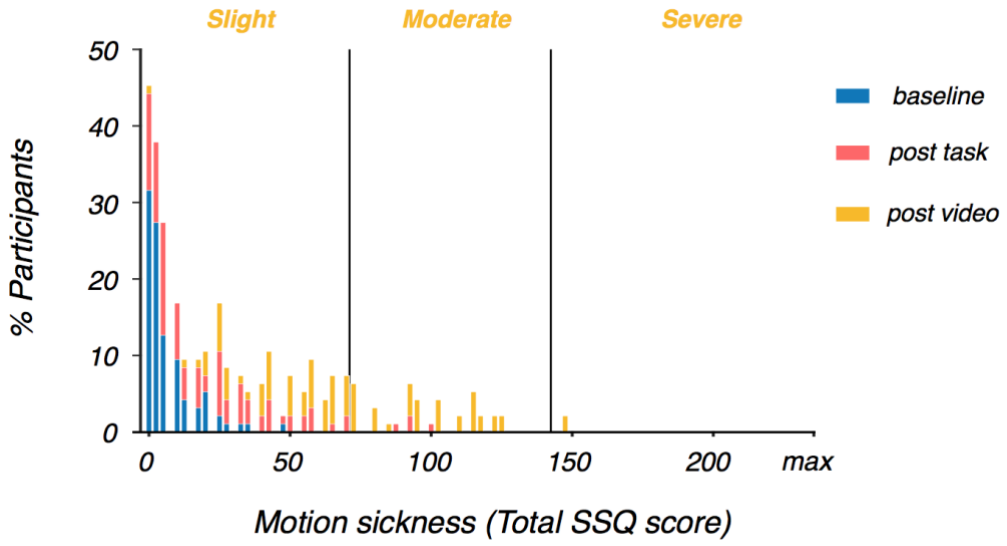

Figure. 4. VR video viewing increased motion sickness. Prior to any VR exposure in the laboratory (baseline - blue bars), observers reported minimal sickness symptoms. Post motion task (i.e., the cue sensitivity assessment - red bars), observers reported slightly elevated sickness symptoms on average. Post video viewing (orange bars), observers reported moderate sickness symptoms on average, as expected. In the analyses reported below, we focused on the change in sickness symptoms directly pre and post video viewing (i.e., post video - post task). The maximum attainable score on the Total SSQ scale is 235.62. See Methods for details.

The increased levels of motion sickness with video viewing were not unexpected given the sensory cue conflicts in the video content. In particular, although care was taken to ensure that the HMD was tailored to the inter-pupillary distance (IPD) of each observer, the binocular disparity in the video content was fixed according to the disparity of the original recording. In addition, the video content lacked motion parallax information since the motion of the camera

used to record the video was inconsistent with the observer's head movement while watching the video.

Sensitivity to 3D Motion Cues Predicts Motion Sickness

We predicted that observers with greater sensitivity to sensory cues would experience more severe motion sickness. Specifically, we hypothesized that sensory cue conflicts give rise to motion sickness, and observers with high sensory sensitivity would be more likely to detect cue conflicts while viewing the VR videos. Thus, when considering the relationship between the motion sickness related to video viewing and sensitivity to the sensory cues, we expected a negative relationship. We found the expected negative relationship in the Full VR condition ($F(1,93) = 9.80$, $p < .001$, $r^2=0.611$; see **Fig. 5).** We did not find a significant relationship between cue sensitivity and motion sickness in any of the other conditions ($p > .0125$, the Bonferroni-corrected alpha-value; see **Table 1**).

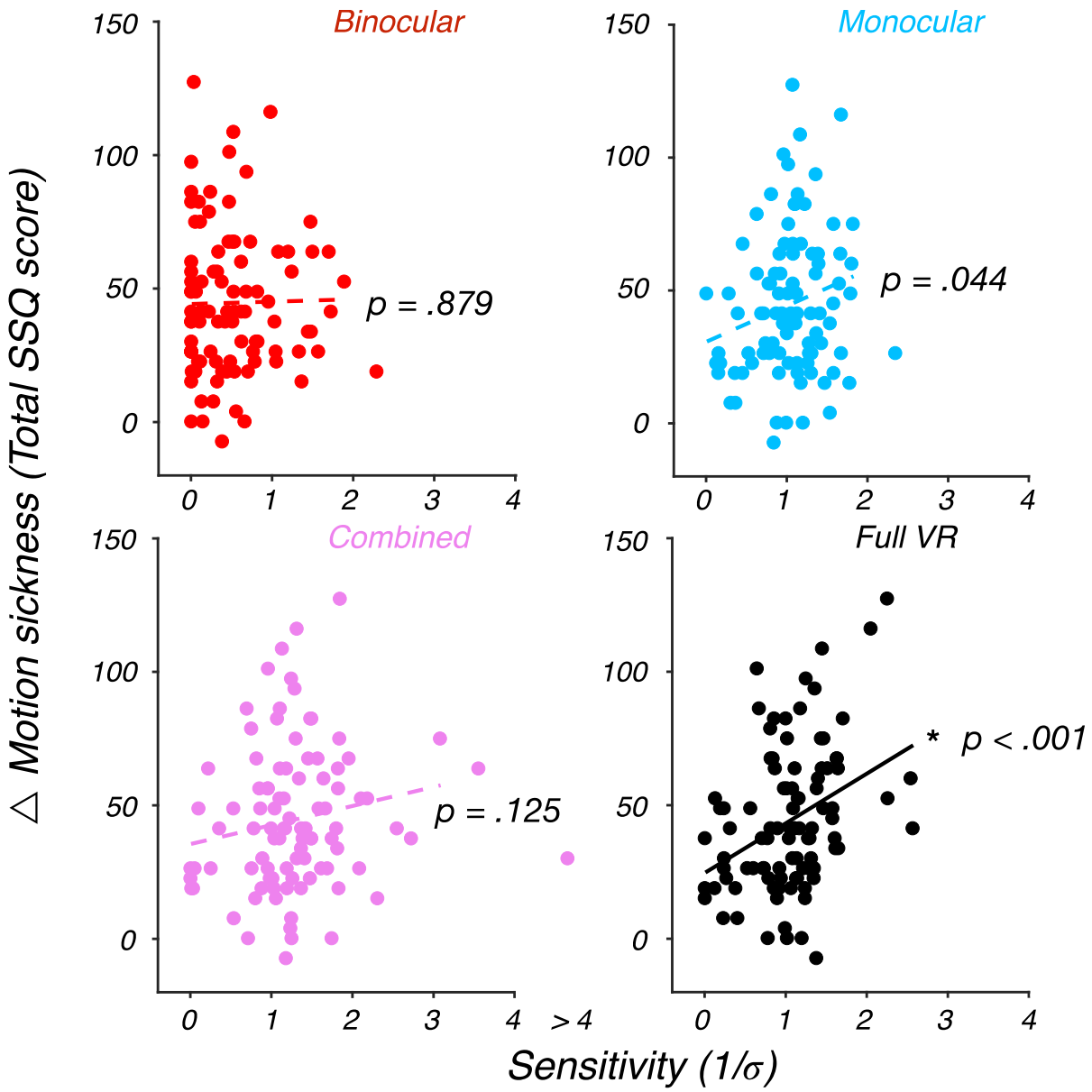

Figure. 5. Sensitivity to motion cues in the Full VR condition predicts motion sickness. For each of the four sensory cue conditions, we computed the relationship between sensitivity to the sensory cues and severity of motion sickness due to video viewing. Solid line denotes a significant relationship at the Bonferroni-corrected alpha level = .0125. The relationship is significant only for the Full VR condition. Given that the Full VR condition is the only of the four sensory cue conditions that contains motion parallax cues, this result suggests that

sensitivity to motion parallax information in particular predicts sickness due to video viewing where motion parallax cues are unavailable.

Cue condition	**Motion sickness (SSQ)**			
	Total sickness	**Nausea**	**Disorientation**	**Oculomotor Discomfort**
Monocular	*p = .044*	*p = .073*	*p = .279*	*p = .029*
Binocular	*p = .879*	*p = .314*	*p = .636*	*p = .906*
Combined (Monocular + Binocular)	*p = .125*	*p = .039*	*p = .556*	*p = .227*
Full VR (Combined + Motion parallax)	****p = .0003***	****p = .00002***	****p = .003***	*p = .041*

****denotes significance at the Bonferroni-corrected alpha level of .0125***

Table 1: Nausea and disorientation in VR are predicted by sensitivity to motion cues in the Full VR condition. Entries correspond to the p-values of the relationships between sensory cue sensitivity in each cue condition and motion sickness due to VR video viewing. Bold p-values with an asterisk denote significance at the Bonferroni-corrected alpha level = .0125. The total sickness score is derived from a combination of the scores on the three separate sub-scales: Nausea, Disorientation, and Oculomotor discomfort. The significant relationship between the total sickness score and sensitivity to the cues in the Full VR condition are primarily driven by Nausea and Disorientation scale symptoms. The trend towards a relationship between the total

sickness score and sensitivity to the cues in the Monocular condition may be primarily driven by Oculomotor discomfort arising from the dot stimulus being visible in only one eye on each trial.

This relationship was specific to two of the three SSQ sub-scales. Sensitivity to the sensory cues in the Full VR condition was highly-correlated with Nausea scale symptoms ($F(1,93) = 19.79, p < .001$) and Disorientation scale symptoms ($F(1,93) = 9.21, p = .003$). No relationship was identified between Full VR sensory cue sensitivity and Oculomotor Discomfort scale symptoms ($p > .0125$, the Bonferroni-corrected alpha-level). We did not find significant relationships between sensitivity to the sensory cues in the Monocular, Binocular, and Combined conditions and these sub-scales ($p > .0125$ in all cases, see **Table 1**).

Our results suggest that sensitivity to motion parallax cues predicts motion sickness. However, our experiments did not test sensitivity to motion parallax in isolation. While it is possible to create stimuli that isolate the monocular and binocular cues, it is not possible to do the same for the motion parallax cues. We therefore computed an index that indirectly quantified an observer's sensitivity to motion parallax cues. Specifically, the index reflected the difference in sensitivity between the Full VR condition and the average of the other three conditions (Monocular, Binocular, and Combined). The results of this analysis confirmed that those with greater sensitivity to motion parallax (i.e., had a positive index value), reported more severe motion sickness symptoms ($F(1,93) = 10.16, p = .002, r_2 = .611$; **Fig. 6**). Taken together, these results confirm the role of cue conflicts in motion sickness, suggesting that observers who rely on motion parallax are more likely to develop sickness symptoms in VR.

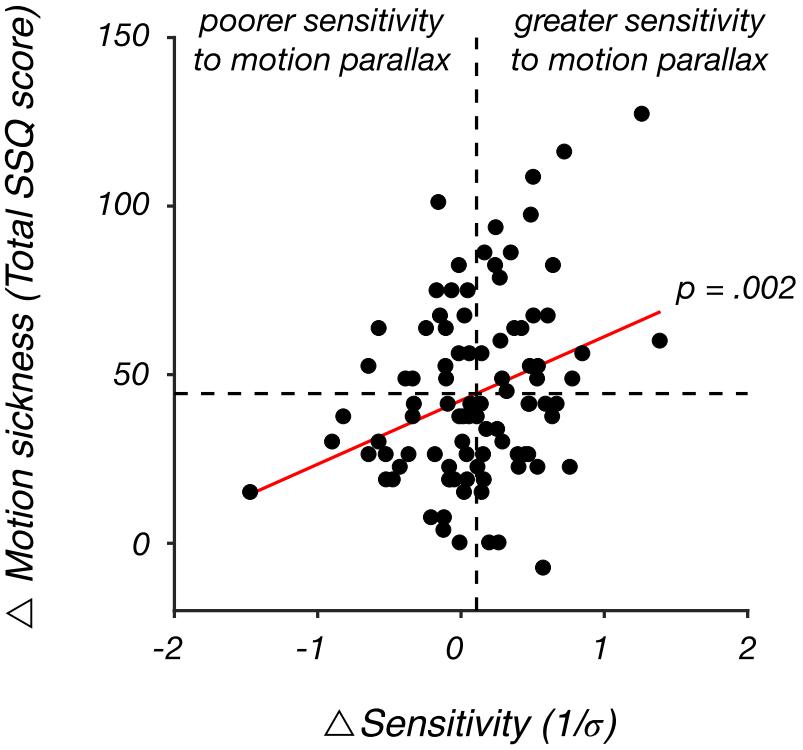

Figure. 6. Sensitivity to motion parallax predicts motion sickness. Delta sensitivity is an index reflecting the difference in sensitivity between the motion parallax-containing Full VR condition and the average sensitivity of the three conditions that do not contain motion parallax information (Monocular, Binocular, and Combined). Positive delta sensitivity values correspond to greater sensitivity to motion parallax information. Solid line denotes significance at the alpha = .05 level. Dashed lines correspond to the between-subject mean delta sensitivity (vertical line) and the between-subject mean change in motion sickness with video viewing (horizontal line), respectively.

No Relationship Between Sex and Motion Sickness

The above analysis indicates that sensitivity to sensory cues, particularly to motion parallax cues, plays a critical role in motion sickness. Previous work has revealed sex differences in susceptibility to motion sickness as well. Specifically, women are thought to be more susceptible to severe motion sickness due to greater postural instability and larger postural sway (Koslucher et al. 2016; Munafo et al. 2017).

We tested for a relationship between sex and motion sickness in addition to the sensitivity to the cues in the Full VR condition. However, we did not find a significant role of role of sex in our data ($F(1,93) = 0.83, p = .36$), nor an interaction between sex and sensitivity in motion sickness ($F(1,93) = 2.61, p = .11$). Finally, the relationship between sensitivity and sickness reported above remained significant when including the sex of the observer in our model ($F(1,93) = 14.91, p < .001$; **Fig. 7**).

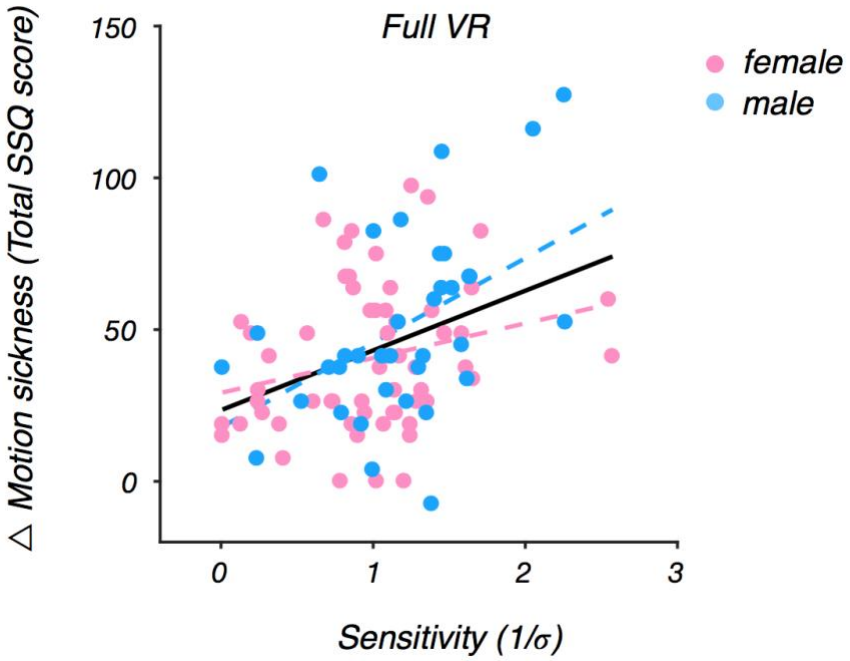

Figure. 7. Motion sickness is predicted by visual sensitivity in Full VR but not sex. The plot depicts the same data as in Fig. 5 - Full VR with sex of the observer denoted. Solid line denotes significance at the alpha = .05 level. The relationship between sensitivity and sickness with effect of sex removed remains significant (solid line), and the effect of sex is not significant. The dashed lines correspond to the sensitivity - sickness relationship for female (pink) and male (blue) observers.

A possible source of discrepancy between current results showing no effect of sex and previous reports may relate to inter-pupillary distance (IPD). Previous studies have largely relied upon a default IPD when presenting experimental stimuli. Default IPDs of stereoscopic stimuli are typically set to 63-64 mm. In the current study, however, we tailored the device to the IPD measurements taken for each observer at the start of the experiment.

Why might this be a source of the difference in sex effects? Consideration of the distribution of IPDs in our sample (see **Fig. 8**) reveals that the average IPD for males is closely-matched to the default device IPD of 64 mm. We should not however that the default IPD still misses the mark for many of the males in our sample. The situation is worse for females, for whom the average IPD is nearly 5 mm smaller than the default IPD. Mismatches between device and observer IPD will inevitably introduce cue conflicts, which will lead to motion sickness. Our results suggest that tailoring the IPD of the display to the individual may reduce motion sickness - that is, ensuring that the IPD of the device is matched to the IPD of the observer will reduce some sources of cue conflicts and will likely eliminate the sex differences reported in previous work.

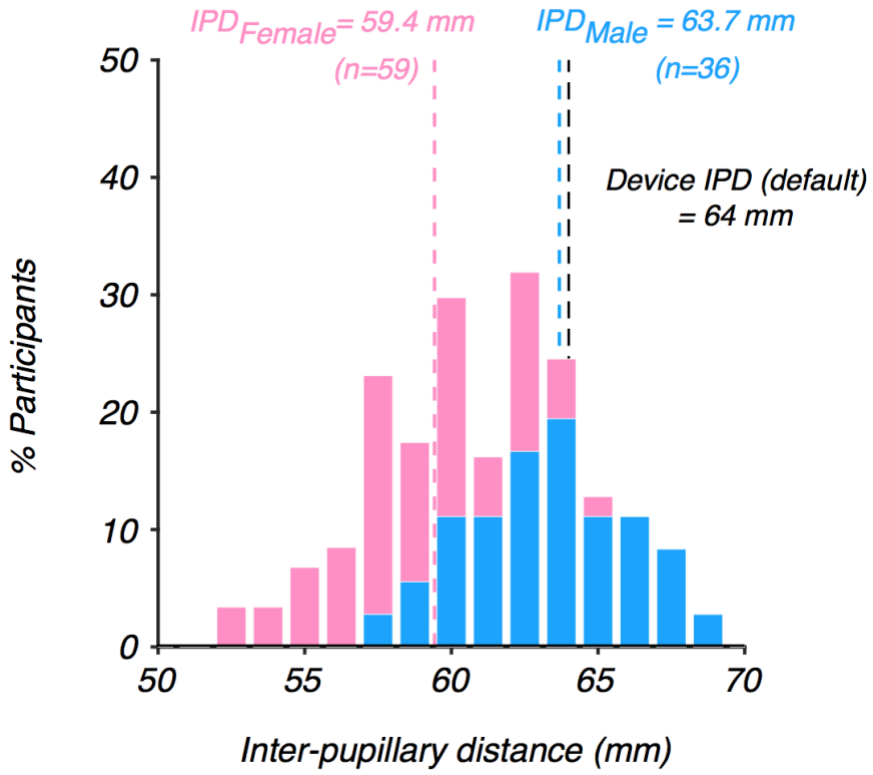

Figure. 8. Inter-pupillary distance (IPD) for the sample of females (pink bars) and males (blue bars) in our experiments. The average male IPD is well-matched to the default IPD of the Oculus DK2, whereas the average female IPD is approximately 5 mm smaller than the default.

One might assume that larger IPDs imply greater sensitivity to binocular cues and hence, that IPD *per se* is an important factor in motion sickness. This assumption is not backed up by our data - no relationship was found between IPD and average sensitivity *($F(1,93) = 0.61$, $p = .44$)*. Moreover, although there was a trend towards individuals with larger IPDs reporting more severe levels of motion sickness due to video viewing, this relationship also did not reach significance *($F(1,93) = 3.82$, $p = .054$)*. Finally, no relationship was found between observer height and motion sickness *($F(1,93) = 0.64$, $p = .43$)*. Therefore, the large variability in

sensitivity to the 3D motion cues measured in our sample must lie in subsequent processing of motion-in-depth signals, not physical characteristics such as IPD or height *per se*.

Observers Reduce Head Movements to Regulate Motion Sickness

If motion sickness is caused by cue conflicts, a useful observer strategy would be to actively eliminate cue conflicts when motion sickness occurs. Since motion parallax-based conflicts appear to be the primary source of motion sickness in VR, observers could eliminate conflict by reducing head movement. This line of reasoning predicts that as individuals start to experience discomfort, they may suppress their head movement. To test whether this strategy is adopted by observers, we analyzed the head movement data collected during the four blocks of the motion task. Note that in three of those blocks, motion parallax cues were absent from the display and were thus in conflict with the parallax cues the observer should expect when they moved their head.

Because the stimuli were presented at fixation for a brief duration (250 ms), observers' head movements were very small (on the order of millimeters and arcmins), and we refer to them as "head jitter". We first analyzed head jitter over the course of an experimental block to determine whether there is evidence of head jitter suppression. We found that on average across observers and experimental blocks, head jitter exhibited a U-shaped pattern: both the magnitude of translational and rotational head jitter declined before rebounding later in the experimental block (see **Fig. 9**). We interpret this pattern as the predicted suppression of head jitter to mitigate motion sickness symptoms, eventually transitioning to a "release" in head jitter once the end of the experimental block is in sight.

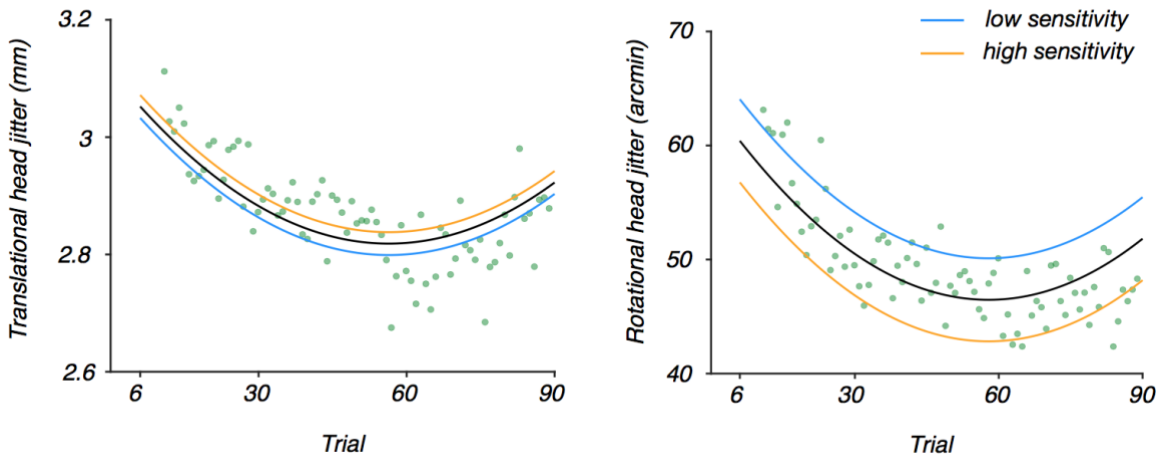

Figure. 9. Modulation of head jitter across trials. For each observer, the average 3D translational head jitter and average 3D rotational head jitter were computed over the four blocks across trials. Data points depict the between-subject average of 3D translational head jitter (left plot) and average 3D rotational head jitter (right plot) across trials. Solid black lines correspond to the quadratic fit to the individual subject data points across trials. Orange lines correspond to fits for a high sensitivity observer whose sensitivity is 1 standard deviation above the mean, and blue lines correspond to fits for a low sensitivity observer whose sensitivity is 1 standard deviation below the mean. The quadratic pattern of both head jitter types indicates that observers suppress head movement over time, which may be used as a strategy to mitigate motion sickness symptoms, and then release head movement during later trials when they likely have experienced a reduction in motion sickness symptoms. Sensitivity to 3D sensory cues significantly modulates the degree of suppression of rotational head jitter only, suggesting that head movements along the rotational axes (i.e., yaw, pitch, and roll) contribute more strongly to motion sickness in VR environments.

We next asked whether the degree of suppression was modulated by an observer's average sensitivity across the four conditions. Specifically, we predicted that observers with greater sensitivity to 3D motion cues would more strongly suppress head jitter. Although translational head jitter exhibited a U-shaped pattern, the effect of sensitivity did not reach significance *($p = .78$)*. However, we did find a significant effect of sensitivity on rotational head jitter ($F(1,7779) = 8.671$, $p = .003$). For every unit increase in an observer's sensitivity, rotational head jitter declined by 9.34 arcmin. This, coupled with the fact that head jitter tended to rebound after the initial suppression suggests that observers dynamically self-regulated their discomfort by reducing their head movement.

Discussion

An attractive aspect of virtual reality (VR) is that it can be used to present visual stimuli under more realistic viewing conditions. However, VR introduces discomfort for an estimated 25-40% of individuals including motion sickness (e.g., Treleaven et al. 2015). In the current study, we have provided evidence that such discomfort arises from sensory cue conflicts, in particular, conflicts related to motion parallax cues.

Importantly, sources of cue conflict are only problematic to the extent that an observer is sensitive to them. Sensitivity to sensory cues in VR was highly-variable across the large sample of observers we studied. Critically, a robust relationship emerged, whereby the greater an observer's sensitivity to motion parallax cues, the more severe the motion sickness symptoms. Indeed, isolating the effects of motion parallax on motion sickness in isolation is not possible in the absence of other cues to 3D motion. However, this finding builds on recent work showing

that sensitivity to 3D motion cues more generally is predictive of motion sickness (Allen et al. 2016) and provides a target for future research on the causes of motion sickness.

Our results also revealed an apparent tendency for observers to self-regulate motion sickness through head movement suppression. Indeed, head movement has previously been implicated in motion sickness. Observers have been shown to decrease head movement in response to sickness-inducing stimuli when exposed to environments with conflicting signals, such as the slow rotation room (SRR; e.g., Reason and Brand, 1975), and in virtual environments (Cobb et al. 1999). Moreover, motion sickness is reduced when the observer's torso or head is restrained (Keshavarz et al. 2017). Future work tracking motion sickness over time at more frequent intervals can confirm head movement reduction as a strategy for self-regulation of motion sickness.

Previous work has shown that rotational movements may play a particular role in motion sickness symptoms due to their role in increasing vection, which causes mismatches between visual and vestibular signals in virtual environments (e.g., So and Lo 1999). Here, we showed that observers in general reduced their head movement in the early portion of each experimental block, followed by a rebound later in the block. Although this pattern was evident in both translational and rotational head movement, rotational head movement suppression was modulated by one's sensitivity to sensory cues. Thus, we have shown that sickness does not arise from head movement *per se*, but rather is related to an observer's sensitivity to sensory cues more generally.

Recent work has also suggested that another factor for motion sickness is an observer's sex (Allen et al. 2016; Koslucher et al. 2016; Munafo et al. 2017). However, we did not find a relationship between sex and motion sickness here. We carefully calibrated the HMD to match

the IPD of each observer rather than relying on a default IPD as has been typical in prior research. As with head movement, our results suggest that it is not one's sex *per se*, but rather poor device calibration that may exacerbate susceptibility to motion sickness.

The current results account for the variability in susceptibility to VR-induced motion sickness across individuals, but imply that those individuals who would benefit the most from the visual cues that can be presented in VR are also those who may experience the most discomfort (Allen et al. 2016).

Our results suggest that motion sickness is not a "necessary evil" of VR technology. A number of strategies can reduce sources of conflict and make the technology more accessible. First, individuals should be encouraged to calibrate the device's assumed IPD prior to VR experiences. Second, head movement monitoring in VR applications may help to identify when observers are starting to feel poorly, upon which the experience can be adjusted (e.g., put up a break screen, downplay the intensity of the game, etc.). Third, VR experiences with modes that require less dramatic head movements by including alternative ways to complete tasks such as "teleporting" rather than navigating may offer more comfortable experiences.
Fourth, experiences in which the intensity of the sickness-inducing cues is gradually increased over multiple exposures, can be an effective way to reduce motion sickness (Graybiel and Wood 1969; Yen Pik et al. 2005). Thus, slowly increasing the intensity of VR exposure may be an important recommendation for new users. Finally, a somewhat counterintuitive option is to make the visual cues that induce motion sickness less reliable, by for example blurring, contrast reduction, or reducing the fidelity of the visual display through other means. Under such conditions observers will downweigh or even completely discount these cues, reducing the cue conflict signals produced by them, and therefore lower their susceptibility to motion sickness.

Acknowledgments

We would like to thank Mohan Ji, Xuanxuan Ge, and Elizabeth Shank for assistance with subject recruitment and data collection and handling.

References

Akiduki, H., Nishiike, S., Watanabe, H., Matsuoka, K., Kubo, T., & Takeda, N. (2003). Visual-vestibular conflict induced by virtual reality in humans. *Neuroscience letters*, *340*(3), 197-200. https://doi.org/10.1016/S0304-3940(03)00098-3

Akizuki, H., Uno, A., Arai, K., Morioka, S., Ohyama, S., Nishiike, S., ... & Takeda, N. (2005). Effects of immersion in virtual reality on postural control. *Neuroscience letters*, *379*(1), 23-26. https://doi.org/10.1016/j.neulet.2004.12.041

Allen, B., Haun, A. M., Hanley, T., Green, C. S., & Rokers, B. (2015). Optimal combination of the binocular cues to 3D motion. *Investigative Ophthalmology & Visual Science*, *56*(12), 7589-7596. https://doi.org/10.1167/iovs.15-17696

Allen, B., Hanley, T., Rokers, B., & Green, C. S. (2016). Visual 3D motion acuity predicts discomfort in 3D stereoscopic environments. *Entertainment computing*, *13*, 1-9. https://doi.org/10.1016/j.entcom.2016.01.001

Beverley, K. I., & Regan, D. (1973). Evidence for the existence of neural mechanisms selectively sensitive to the direction of movement in space. *The Journal of physiology*, *235*(1), 17-29. https://doi.org/10.1113/jphysiol.1973.sp010376

Brainard, D. H. (1997). The psychophysics toolbox. *Spatial vision*, *10*(4), 433-436. https://doi.org/10.1163/156856897X00357

Brenner, E., Van Den Berg, A. V., & Van Damme, W. J. (1996). Perceived motion in depth. *Vision research*, *36*(5), 699-706. https://doi.org/10.1016/0042-6989(95)00146-8

Bronstein, A. M., Golding, J. F., & Gresty, M. A. (2013, July). Vertigo and dizziness from environmental motion: visual vertigo, motion sickness, and drivers' disorientation. In *Seminars in neurology* (Vol. 33, No. 03, pp. 219-230). Thieme Medical Publishers. https://doi.org/10.1055/s-0033-1354602

Cobb, S. V., Nichols, S., Ramsey, A., & Wilson, J. R. (1999). Virtual reality-induced symptoms and effects (VRISE). *Presence: Teleoperators & Virtual Environments*, *8*(2), 169-186. https://doi.org/10.1162/105474699566152

Fulvio, J. M., & Rokers, B. (2017). Use of cues in virtual reality depends on visual feedback. *Scientific reports*, *7*(1), 1-13. https://doi.org/10.1038/s41598-017-16161-3

Graybiel, A., & Wood, C. D. (1968). *Rapid vestibular adaptation in a rotating environment by means of controlled head movements Aerospace Medicine, 40(6), 638–643.* https://doi.org/10.1037/e460462004-001

Hill, K. J., & Howarth, P. A. (2000). Habituation to the side effects of immersion in a virtual environment. *Displays*, *21*(1), 25-30. https://doi.org/10.1016/S0141-9382(00)00029-9

Howarth, P. A., & Costello, P. J. (1997). The occurrence of virtual simulation sickness symptoms when an HMD was used as a personal viewing system. *Displays*, *18*(2), 107-116. https://doi.org/10.1016/S0141-9382(97)00011-5

Graybiel, A., & Kennedy, R. S. (1965). The Dial Test-A standardized procedure for the experimental production of canal sickness symptomatology in a rotating environment. *Naval School of Aviation Medicine Pensacola FL.* Retrieved from http://www.dtic.mil/docs/citations/AD0625863. https://doi.org/10.21236/AD0625863

Kennedy, R. S., Lane, N. E., Berbaum, K. S., & Lilienthal, M. G. (1993). Simulator sickness questionnaire: An enhanced method for quantifying simulator sickness. *The international journal of aviation psychology*, *3*(3), 203-220. https://doi.org/10.1207/s15327108ijap0303_3

Keshavarz, B., Hecht, H., & Zschutschke, L. (2011). Intra-visual conflict in visually induced motion sickness. *Displays*, *32*(4), 181-188. https://doi.org/10.1016/j.displa.2011.05.009

Keshavarz, B., Novak, A. C., Hettinger, L. J., Stoffregen, T. A., & Campos, J. L. (2017). Passive restraint reduces visually induced motion sickness in older adults. *Journal of experimental psychology: Applied*, *23*(1), 85-99. https://doi.org/10.1037/xap0000107

Kleiner, M., Brainard, D., & Pelli, D. (2007). What's new in Psychtoolbox-3?. *Perception, 36(14), 1*.

Koslucher, F., Munafo, J., & Stoffregen, T. A. (2016). Postural sway in men and women during nauseogenic motion of the illuminated environment. *Experimental brain research*, *234*(9), 2709-2720. https://doi.org/10.1007/s00221-016-4675-8

Lackner, J. R. (2014). Motion sickness: more than nausea and vomiting. *Experimental brain research*, *232*(8), 2493-2510. https://doi.org/10.1007/s00221-014-4008-8

LaViola, J. J. (2000). A discussion of cybersickness in virtual environments. *ACM Sigchi Bulletin*, *32*(1), 47-56. https://doi.org/10.1145/333329.333344

Money, K. (1990). Motion sickness and evolution. *Motion and space sickness (A 93-55929 24-52). Boca Raton, FL, CRC Press, Inc.*, *1990*, 1-7.

Munafo, J., Diedrick, M., & Stoffregen, T. A. (2017). The virtual reality head-mounted display Oculus Rift induces motion sickness and is sexist in its effects. *Experimental brain research*, *235*(3), 889-901. https://doi.org/10.1007/s00221-016-4846-7

Nachum, Z., Shupak, A., Letichevsky, V., Ben-David, J., Tal, D., Tamir, A., ... & Luntz, M. (2004). Mal de debarquement and posture: reduced reliance on vestibular and visual cues. *The Laryngoscope*, *114*(3), 581-586. https://doi.org/10.1097/00005537-200403000-00036

Nefs, H. T., O'Hare, L., & Harris, J. M. (2010). Two independent mechanisms for motion-in-depth perception: Evidence from individual differences. *Frontiers in Psychology*, *1*, 155. https://doi.org/10.3389/fpsyg.2010.00155

Nishiike, S., Okazaki, S., Watanabe, H., Akizuki, H., Imai, T., Uno, A., ... & Inohara, H. (2013). The effect of visual-vestibulosomatosensory conflict induced by virtual reality on postural stability in humans. *The Journal of Medical Investigation*, *60*(3.4), 236-239. https://doi.org/10.2152/jmi.60.236

Oman, C. M. (1990). Motion sickness: a synthesis and evaluation of the sensory conflict theory. *Canadian journal of physiology and pharmacology*, *68*(2), 294-303. https://doi.org/10.1139/y90-044

Paillard, A. C., Quarck, G., Paolino, F., Denise, P., Paolino, M., Golding, J. F., & Ghulyan-Bedikian, V. (2013). Motion sickness susceptibility in healthy subjects and vestibular patients: effects of gender, age and trait-anxiety. *Journal of Vestibular Research*, *23*(4, 5), 203-209. https://doi.org/10.3233/VES-130501

Pelli, D. G. (1997). The VideoToolbox software for visual psychophysics: Transforming numbers into movies. *Spatial vision*, *10*(4), 437-442. https://doi.org/10.1163/156856897X00366

Reason, J. T., & Brand, J. J. (1975). *Motion sickness*. *Academic press.*

Reason, J. T. (1978). Motion sickness adaptation: a neural mismatch model. *Journal of the Royal Society of Medicine*, *71*(11), 819-829. https://doi.org/10.1177/014107687807101109

Riccio, G. E., & Stoffregen, T. A. (1991). An ecological theory of motion sickness and postural instability. *Ecological psychology*, *3*(3), 195-240. https://doi.org/10.1207/s15326969eco0303_2

Smart, L. J., Stoffregen, T. A., & Bardy, B. G. (2002). Visually induced motion sickness predicted by postural instability. *Human factors*, *44*(3), 451-465. https://doi.org/10.1518/0018720024497745

So, R. H., & Lo, W. T. (1999, March). Cybersickness: an experimental study to isolate the effects of rotational scene oscillations. In *Proceedings IEEE Virtual Reality (Cat. No. 99CB36316)* (pp. 237-241).

Stoffregen, T. A., Faugloire, E., Yoshida, K., Flanagan, M. B., & Merhi, O. (2008). Motion sickness and postural sway in console video games. *Human factors*, *50*(2), 322-331. https://doi.org/10.1518/001872008X250755

Treisman, M. (1977). Motion sickness: an evolutionary hypothesis. *Science*, *197*(4302), 493-495. https://doi.org/10.1126/science.301659

Treleaven, J., Battershill, J., Cole, D., Fadelli, C., Freestone, S., Lang, K., & Sarig-Bahat, H. (2015). Simulator sickness incidence and susceptibility during neck motion-controlled virtual reality tasks. *Virtual Reality*, *19*(3-4), 267-275. https://doi.org/10.1007/s10055-015-0266-4

Yen Pik Sang, F., Billar, J., Gresty, M. A., & Golding, J. F. (2005). Effect of a novel motion desensitization training regime and controlled breathing on habituation to motion sickness. *Perceptual and Motor Skills, 18*(1), 29-34. https://doi.org/10.2466/pms.101.1.244-256